AQAM under high time delay spread conditions

SHAN Xiao-hong (单晓红), ZHU Xiu-shan (朱秀珊), GUO Yin-jing (郭银景), LIU Zhi-wen (刘治文)
(*College of Information and Electrical Engineering, Shandong University of Science and Technology, Qingdao 266510, China*)

Abstract: An analysis process is described for adaptive quadrature amplitude modulation (AQAM) of constant-power constant-symbol-rate over frequency-selective Rayleigh fading channels with inter symbol interference (ISI) and Gaussian noise. The delay spread resistance of the AQAM scheme is put forward by studying its average throughput and average bit-error-rate (BER), both of which can be expressed as functions of two variables, the ratio of root mean square (RMS) delay spread to symbol period and the ratio of average symbol energy to noise. Average throughput reacts regularly to the latter, whereas it does not react to the former. The AQAM scheme is highly superior in the delay spread resistance in comparison with the fixed modulation modes. Gains of the AQAM scheme over the fixed modes become more significant as the delay spread becomes severer or the average throughput decreases.

Key words: time delay spread; adaptive modulation; adaptive quadrature amplitude modulation (AQAM)

CLD number: TN929.5 **Document code:** A
Article ID: 1674-8042(2012)02-0152-05 **doi:** 10.3969/j.issn.1674-8042.2012.02.011

Adaptive modulation, which has been widely studied, is a promising technique providing a higher data rate in wireless communications. For example, Ref.[1] discussed the effects of channel prediction; Refs.[2] and [3] investigated rake-receiver-assisted adaptive modulation[4]; Ref.[4] derived a set of optimal switching levels. However, little research has been done on the delay spread immunity of adaptive modulation. The delay spread immunity of the fixed modulation modes was studied in Refs.[5] and [6]. Ref.[7] investigated a variable-symbol-rate adaptive modulation scheme by doing simulations under particular conditions in high delay spread environments. In this work, constant-power constant-symbol-rate adaptive quadrature amplitude modulation (AQAM) is analyzed over frequency-selective Rayleigh fading channels with inter symbol interference (ISI) and Gaussian noise, and how the average bit-error-rate (BER) and average throughput of the AQAM scheme react to the delay spread is investigated.

1 Instantaneous signal to noise and interference ratio

We use $h(t)$ to represent impulse response of the frequency-selective fading channel, and $g_{tr}(t)$ and $g_{rec}(t)$ impulse responses of the transmitting filter and the receiving filter respectively. The convolution $g_{tr}(t) * g_{rec}(t) = g(t)$ results in a raised cosine spectrum with a rolloff factor α; their Fourier transforms satisfy[8]

$$G_{tr}(f) = G_{rec}(f) = \sqrt{G(f)}. \tag{1}$$

We set $\alpha = 5$ in this research, but the analysis procedure described here can be readily applied to $0 < \alpha \leqslant 1$. Let $\{X_n\}$ represent the sequence of symbols, and then the average symbol energy can be given by

$$E_{sav} = \frac{1}{2}E[|X_n|^2]. \tag{2}$$

Output of the receiving filter is

$$r(t) = \sum_n X_n q(t - nT_s) + v(t), \tag{3}$$

where $q(t) = g(t) * h(t)$, T_s is symbol period and $v(t)$ is zero-mean Gaussian noise with autocorrelation function $\varphi_{vv}(\tau) = N_0\delta(\tau)$. For symbol X_n, $r(t)$ is sampled at $t = nT_s + t_d$, where timing delay t_d is calculated by using the method presented in Ref.[9]. The detection sample for X_0 can be given as

$$U_0 = X_0|q(t_d)|^2 + \sum_{n\neq 0} X_n q(t_d - nT_s)q^*(t_d) + v(t_d)q^*(t_d) = X_0 z + I(t_d) + N(t_d), \tag{4}$$

where $z = |q(t_d)|^2$, $q^*(t_d)$ is the complex conjugate of $q(t_d)$, and $I(t_d)$ and $N(t_d)$ denote the ISI

* Received data: 2011-11-12
Foundation item: National Natural Science Foundation of China (No. 61071087); Research contract from Shandong University of Science and Technology (Chun Lei 2009BWZ037)
Corresponding author: SHAN Xiao-hong (xiaoshanhong@163.com)

term and the noise term respectively.

When square QAM modes are used, $\{X_n\}$ is complex-valued, and the instantaneous signal to noise and interference ratio (SNIR) per symbol γ can be expressed as

$$\gamma = \frac{z^2 E[|X_0|^2]}{E[|I(t_d)|^2] + E[|N(t_d)|^2]}, \quad (5)$$

where

$$E[|N(t_d)|^2] = 2N_0 z, \quad (6)$$

and according to Ref.[9],

$$E[|I(t_d)|^2] = z^2 E[|X_n|^2] \sum_{n\neq 0} R_n^2 + 2zE[|X_n|^2] \sum_{n\neq 0} \sigma_n^2, \quad (7)$$

where R_n and σ_n^2 are defined as

$$R_n = E[q_c(t_d - nT_s) q_c(t_d)] / E[q_c^2(t_d)], \quad (8)$$

$$\sigma_n^2 = \frac{1}{2}(E[|q(t_d - nT_s)|^2] - E[|q(t_d)|^2] R_n^2). \quad (9)$$

In Eq.(8), $q_c(t_d)$ and $q_c(t_d - nT_s)$ denote the real parts of $q(t_d)$ and $q(t_d - nT_s)$. Substituting Eqs.(2), (6) and (7) into Eq.(5) then

$$\gamma(z \mid d, E_{sav}/N_0) = \frac{z}{C_a z + C_b + C_c}, \quad (10)$$

where d is the normalized RMS delay spread, defined as $d = \tau_{rms}/T_s$, where τ_{rms} is the RMS delay spread, and

$$C_a = \sum_{n\neq 0} R_n^2,\ C_b = 2\sum_{n\neq 0} \sigma_n^2,\ C_c = N_0/E_{sav}.$$

As timing delay t_d is a function of τ_{rms}[9], C_a and C_b are functions of the normalized RMS delay spread d according to definitions of R_n and σ_n^2. Therefore, the instantaneous SNIR γ can be treated as a function of z, and the function is conditioned on d and E_{sav}/N_0. We observe from Eq.(10) that $0 \leqslant \gamma < 1/G_a$ at a given d and E_{sav}/N_0.

When binary phase shift keying (BPSK) mode is used, the sequence $\{X_n\}$ is real-valued and in Eq.(4), only the real parts of $I(t_d)$ and $N(t_d)$ need to be considered. In this case, the instantaneous SNIR γ is given by

$$\gamma(z \mid d, E_{sav}/N_0) = \frac{z}{2C_a z + C_b + C_c}, \quad (11)$$

where $0 \leqslant \gamma < 1/(2C_a)$ at a given d and E_{sav}/N_0.

2 Definition of average throughput and average BER

At first, we consider a simple multipath Rayleigh fading channel model, two-ray Rayleigh fading channel, whose impulse response is given by[5]

$$h(t) = (h_{1c} + jh_{1s})\delta(t) + (h_{2c} + jh_{2s})\delta(t - \tau), \quad (12)$$

where τ is the delay between two rays and h_{1c}, h_{1s}, h_{2c}, h_{2s} are zero-mean independent Gaussian random variables, each having a 0.25 variance. Thus we have $\tau_{rms} = \tau/2$ and

$$z = |q(t_d)|^2 = [h_{1c} g(t_d) + h_{2c} g(t_d - \tau)]^2 + [h_{1s} g(t_d) + h_{2s} g(t_d - \tau)]^2. \quad (13)$$

From Eq.(13), it can be seen that z is determined exclusively by the instantaneous channel conditions $\{h_{1c}, h_{1s}, h_{2c}, h_{2s}\}$ at a given d.

As the instantaneous SNIR γ has different expressions for square QAM than for BPSK, we employ z as the channel quality measure, which is independent of the modulation modes. We observe from Eq.(13) that z is chi-square distributed with two degrees of freedom; its probability density function (PDF) can be given by

$$p_z(z) = \frac{1}{W} e^{-z/W},\ z \geqslant 0, \quad (14)$$

where $W = [g^2(t_d) + g^2(t_d - \tau)]/2$.

We study constant-power constant-symbol-rate AQAMs, for which the symbol period T_s and symbol energy E_{sav} are fixed. In the AQAM system with K modes, b_k denotes the bits per symbol (BPS) of mode k ($k = 0, 1, \cdots, K-1$). Let $\{l_0, l_1, \cdots, l_K\}$ be the set of switching levels, where $l_0 = 0$ and $l_K = +\infty$. $l_k \leqslant z < l_{k+1}$ mode k is chosen for transmission. When mode k is used, the instantaneous BER is given by[4]

$$\mathrm{IBER}_k(\gamma) = \sum_j A_{k,j} Q(\sqrt{a_{k,j}\gamma}), \quad (15)$$

where $\{A_{k,j}, a_{k,j}\}$ is a set of mode dependent constants[4].

We investigate the average spectral efficiency (expressed in terms of bps/Hz) of the AQAM scheme through its average BPS, which is in direct proportion to the former when the rolloff factor α is fixed. The average BPS and the average BER for the AQAM scheme can be expressed as

$$B(d, E_{sav}/N_0) = \sum_{k=0}^{K-1} b_k \int_{l_k}^{l_{k+1}} p_z(z) dz = \sum_{k=0}^{K-1} b_k [\exp(-l_k/W) - \exp(-l_{k+1}/W)], \quad (16)$$

$$\overline{\mathrm{BER}}(d, E_{sav}/N_0) = \frac{\sum_{k=0}^{K-1} b_k \int_{l_k}^{l_{k+1}} \mathrm{IBER}_k(\gamma) p_z(z) \mathrm{d}z}{B(d, E_{sav}/N_0)}. \quad (17)$$

Average BER constraint is applied in this study; BET_T denotes the target BER. Using the method presented in Ref.[4], we find the optimal switching levels, which can maximize the average BPS while maintaining $BER(d, E_{sav}/N_0) \leqslant BER_T$ for any given d and E_{sav}/N_0. The set of optimal switching levels is varied depending on d and E_{sav}/N_0.

3 Five-mode AQAM performance

Five modes are employed for the AQAM scheme. Mode 0, 1, 2, 3 and 4 refer to no transmission, BPSK, QPSK, 16QAM, 64QAM respectively when the case $BET_T = 10^{-3}$ is studied.

Let thr_k represent the instantaneous SNIR value that is required by mode $k(k=1,2,3,4)$ for obtaining the instantaneous BER of 10^{-3}. We obtain from (15) that thr_1 = 6.79 dB, thr_2 = 9.8 dB, thr_3 = 16.54 dB, thr = 22.55 dB. As $0 \leqslant \gamma < 1/(2C_a)$ for BPSK, we have $IBET_1(\gamma) > 10^{-3}$ for all γ when $thr_k \geqslant 1/(C_a)$, and similarly, $IBET_k(\gamma) > 10^{-3}$ for all γ when $thr_k \geqslant 1/C_a(k=2,3,4)$. Since C_a is a function of the normalized rms delay spread d, at first, we need to decide the range of d, where the corresponding values of C_a make $BER(d, E_{sav}/N_0) \leqslant 10^{-3}$ possible.

Fig.1 illustrates $1/(2C_a)$ and $1/C_a$ for $0<d<0.5$.

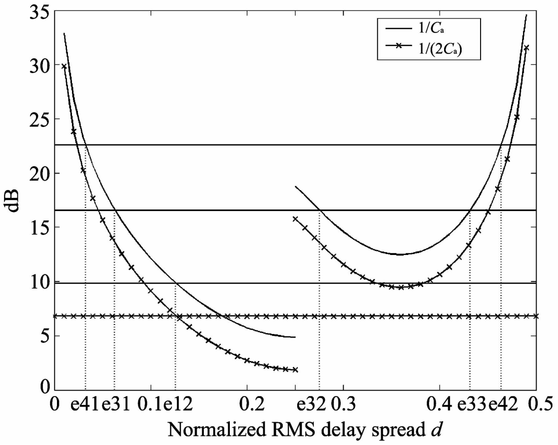

Fig.1 $1/C_a$ and $1/(2C_a)$ as functions of normalized rms delay spread d

In Fig.1, the two curves are monotonic decreasing for $0<d<0.25$ and only left continuous at $d=0.25$. Four lines parallel to the X axis and with ordinates thr_1, thr_2, thr_3 shown in Fig.1. The line thr_4 crosses the curve $1/C_a$ at two points, the abscissas of which are denoted by $e41$ and $e42$; When line thr_3 at three points, the abscissas are $e31$, $e32$ and $e33$; When line thr_2 one point, the abscissa is $e2$. Line crosses the curve$1/(2C_a)$ at one point whose abscissa is denoted by $e1$. It should be noted that $e2 = e1$, because is twice of thr_1. We use $e12$ to represent $e2$ and $e1$ to obtain $e41 \approx 0.032$, $e42 \approx 0.464$, $e3 \approx 10.063$, $e32 \approx 0.276$, $e33 \approx 0.432$, $e12 \approx 0.126$ with help of the graphical method. We observe from Fig.1 that when $e12 \leqslant d \leqslant 0.25$, $IBET_k(\gamma) > 10^{-3}$ is true for all γ and all modulation modes. Therefore, the average BER of 10^{-3} cannot be achieved in range $e12 \leqslant d \leqslant 0.25$. However, it is possible in ranges $0<d<e12$ and $0.25<d<0.5$. Then, the average BER and average BPS are investigated in the two ranges.

3.1 Average BER

When $d \leqslant 0.01$, fixed 64QAM mode is able to obtain 10^{-3} average BER, whereas when $d \geqslant 0.02$ its irreducible average BER is higher than 10^{-3}. Under average BER constraint, for a given $d \leqslant 0.01$, average BER of the AQAM scheme $BER(d, E_{sav}/N_0)$ is a constant at 10^{-3} until E_{sav}/N_0 increases to threshold for fixed 64QAM mode obtaining lower than 10^{-3} average BER, and then the AQAM scheme begins to function as fixed 64QAM mode. For $0.02 \leqslant d < e12$ and $0.25<d<0.5$, $BER(d, E_{sav}/N_0) = 10^{-3}$ regardless of d and E_{sav}/N_0.

3.2 Average BPS for $0<d<e12$

The average BPS $B(d, E_{sav}/N_0)$ is depicted as a function of E_{sav}/N_0 for different values of d (Fig.2(a)), where eight curves are plotted in order not to crowd the graph. The average BPS as E_{sav}/N_0 approaching infinite $B_{Inf}(d)$ is shown in Fig.2(b).

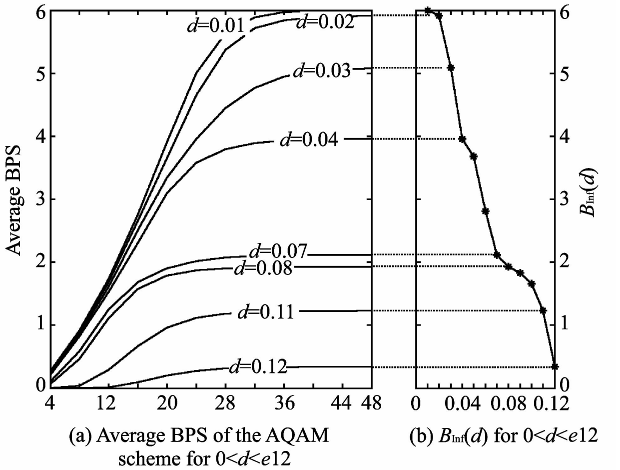

Fig.2 BPS performance for $0<d<e12$

Observing Fig.2, we find that all curves approach saturation points when E_{sav}/N_0 = 48 dB. AQAM scheme can achieve the average BPS of 1 when $d \leqslant 0.11$; 2, when $d \leqslant 0.07$; 4, when $d \leqslant 0.03$; 6, when $d \leqslant 0.01$. By contrast, fixed BPSK mode cannot obtain the average BER of 10^{-3} when $d > 0.05$;

the fixed QPSK when $d \geqslant 0.04$; fixed 16QAM when $d \geqslant 0.02$.

Table 1 summarizes the E_{sav}/N_0 gain that AQAM scheme achieves over fixed modes under the average BER of 10^{-3} and the same (average) BPS. Table 1 shows that the gains are significant, which increase with the normalized rms delay spread d and decrease statistically when the (average) BPS increases. When the (average) BPS is 6, there are no gains.

Table 1 Gains of AQAM scheme over fixed modes under the average BER of 10^{-3} and the same (average) BPS

d	Required E_{sav}/N_0 (dB) for the average BER of 10^{-3}		Gain /dB
	(Average) BPS = 1		
	AQAM	BPSK	
0.01	8.45	24.12	15.67
0.02	8.55	24.65	16.1
0.03	8.73	25.74	17.01
0.04	8.98	28.14	19.16
0.05	9.33	–	–
	(Average) BPS = 2		
	AQAM	QPSK	
0.01	13.12	27.28	14.16
0.02	13.37	28.38	15.01
0.03	13.82	31.41	17.59
0.04	14.55	–	–
	(Average) BPS = 4		
	AQAM	QPSK	
0.01	20.29	34.32	14.03
0.02	21.36	–	–
	(Average) BPS = 6		
	AQAM	QPSK	
0.01	48	48	–

3.3 Average BPS for $0.25 < d < 0.5$

In view of bad performance in the range $0.34 \leqslant d < 0.5$, where $B_{Inf}(d) < 0.1$, we concentrate on $0.25 < d \leqslant 0.33$, where the average BPS $B(d, E_{sav}/N_0)$ reacts to d and E_{sav}/N_0 as it does in Fig. 2(a). Fig. 3 depicts $B_{Inf}(d) = 1.19$ for $0.25 < d \leqslant 0.33$. We have $B_{Inf}(d) = 1.19$ as d approaches 0.25 and $B_{Inf}(d) < 1$ when $d > 0.27$.

We observe from Fig. 2(b) and Fig. 3 that $B_{Inf}(d)$ decreases monotonically as d increases for $0 < d < e12$ as well as for $0.25 < d \leqslant 0.33$, but this is not true from perspective of the overall range of $0 < d < 0.33$. For example, $B_{Inf}(0.31) > B_{Inf}(0.12)$. This can be explained by Fig. 4, where the parameters C_a, C_b and W are illustrated for $0 < d < 0.33$. We have two observations from Fig. 4: 1) None of the three curves are continuous at $d = 0.25$, which results from discontinuity of the timing delay t_d at $d = 0.25$[9]; 2) Respective trends of the three curves for $0 < d < 0.25$ are similar to those for $0.25 < d < 0.33$. The two points lead to the irregular behavior of $B_{Inf}(d)$, including that for $e12 \leqslant d \leqslant 0.25$. We consider $B_{Inf}(d) = 0$ for $e12 \leqslant d \leqslant 0.25$.

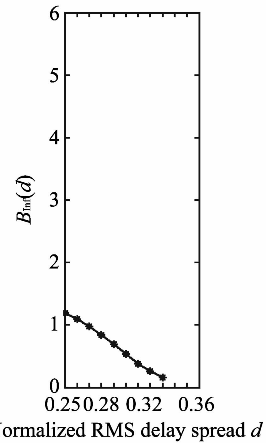

Fig. 3 $B_{Inf}(d)$ for $0.25 < d \leqslant 0.33$

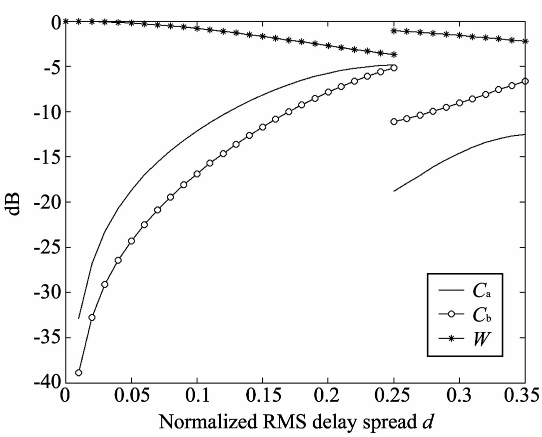

Fig. 4 C_a, C_b and W as functions of normalized RMS delay spread d

The results we have obtained for $0 < d < 0.126$ hold true for other channel models, because the effects of delay spectrum shape on performances can be neglected when $d < 0.2$[9]. The results we have obtained for $0.25 < d < 0.5$ can be regarded as lower bounds on the performances, because the two-ray channel model we use, whose two rays have equal power, represents an extremely unfavorable transmission environment.

4 Conclusions and other considerations

Compared to the fixed modes, AQAM scheme is highly superior in the delay spread resistance, especially under severer delay spread and lower throughput.

As normalized rms delay spread d increases, the average BPS does not decrease monotonically for overall range of $0<d<0.5$.

When $d<0.27$, it is possible for AQAM scheme to achieve an average BPS between 1 and 6 while providing an 10^{-3} average BER.

Although the rolloff factor α is fixed at 0.5 in this study, the analysis procedure described in this research can be readily applied to any $0<\alpha\leqslant 1$.

Resistance to delay spread can be increased by using an even higher α, which, however, will cause a wider transmission bandwidth. We will investigate the trade-off between delay spread resistance and spectral efficiency (in terms of bps/Hz) as an extension of this work. In addition, we will find the details about how the delay spread resistance of AQAM scheme depends on delay spectrum shape when the normalized rms delay spread d exceeds 0.2.

References

[1] Falahati S, Svensson A, Ekman T, et al. Adaptive modulation systems for predicted wireless channels. IEEE Trans. on Communication, 2004, 52(2):307-316.

[2] Choi B J, Munster M, Yang L L, et al. Performance of rake receiver assisted adaptive-modulation based CDMA over frequency selective slow Rayleigh fading channels. Electronics Letters, 2001, 37(4):247-249.

[3] Kim J, Kim I, Ro S, et al. Effects of multipath diversity on adaptive QAM in frequency selective Rayleigh fading channels. IEEE Communications Letters, 2002, 6(9): 364-366.

[4] Choi B, Hanzo L. Optimum mode-switching-assisted constant-power single- and multicarrier adaptive modulation. IEEE Trans. on Vehicular Technology, 2003, 52(3):536-560.

[5] Fung V, Rappaport T S, Thoma B. Bit error simulation for /4 DQPSK mobile radio communications using Two-Ray and measurement-based impulse response models. IEEE Journal of Selection Areas Communication, 1993, 11(3):393-405.

[6] Chuang J C-I. The effects of time delay spread on portable radio communications channels with digital modulation. IEEE Journal of Selection Areas Communications, 1987, 5(5): 879-889.

[7] Ue T, Sampei S, Morinaga N. Symbol rate and modulation level controlled adaptive modulation system with TDMA/TDD for high bit rate transmission in high delay spread environments. Electronics Letters, 1996, 32(4): 304-305.

[8] Rappaport T S. Wireless communications principles and practice, Prentice-Hall, 1996.

[9] Glance B, Greenstein L J. Frequency-selective fading effects in digital mobile radio with diversity combining. IEEE Trans. on Communications. 1983, 31(9): 1085-1094.